Surface & Coatings Technology 368 (2019) 192–201

Contents lists available at ScienceDirect

Surface & Coatings Technology

journal homepage: www.elsevier.com/locate/surfcoat

Highly oxidation resistant MCrAlY bond coats prepared by heat treatment under low oxygen content

Guo-Hui Meng, Hong Liu, Mei-Jun Liu, Tong Xu, Guan-Jun Yang*, Cheng-Xin Li, Chang-Jiu Li

State Key Laboratory for Mechanical Behavior of Materials, School of Materials Science and Engineering, Xi'an Jiaotong University, Xi'an, Shaanxi 710049, PR China

ARTICLE INFO

Keywords:
Heat treatment
Thermal barrier coatings
High temperature oxidation
Thermally grown oxide
MCrAlY bond coat
Surface microstructure

ABSTRACT

High-performance gas turbines and aircraft engines require high oxidation resistance MCrAlY bond coats. In this study, a novel heat treatment under low oxygen content was developed to prepare highly oxidation resistant MCrAlY bond coats. The results showed that after the heat treatment, metallic phases without as-deposited alumina film were exposed on the MCrAlY bond coat surface. The α-Al_2O_3 thermally grown oxide (TGO) with a larger grain size was formed on the heat-treated bond coat surface during isothermal oxidation. This larger α-Al_2O_3 TGO grain size significantly inhibited the TGO layer growth of MCrAlY bond coats by 2.7 times.

1. Introduction

Thermal barrier coatings (TBCs) are an essential component for improving the thrust ratio and efficiency of aircraft engines and gas turbines [1–4]. The use of TBCs, along with the internal cooling of underlying metal components, provides major increases in the operating temperatures of engines. This enables modern engines to operate at gas temperatures well above the melting temperature of metal components, thereby improving the efficiency of engines [2,5]. Today, the advanced TBCs for industrial applications are typically composed of a nickel- or cobalt-based superalloy substrate, a thermally grown oxide (TGO) layer, a MCrAlY (M is Ni, Co, or a mixture of Ni and Co) bond coat, and an Y_2O_3 stabilized ZrO_2 (YSZ) top coat [1–9]. The MCrAlY bond coat is designed to protect the substrate from corrosion and oxidation by forming the protective TGO layer on its surface, while the YSZ top coat is used for heat insulation [2,5]. In general, every layer of the TBCs has an important effect on the service life of engines, since failure of any layer can lead to premature failure of TBCs, which exposes the metal components of engines to harsh environments [2,10,11]. It is worth noting that during the laboratory testing and the practical engine service, the spallation and delamination of the YSZ top coat near the TGO layer is the typical failure mode of the TBCs [2,12,13]. Although there are many factors that contribute to the failure of the YSZ top coat, it is generally believed that the most important factor is the TGO layer growth [2,13]. The rapid growth of TGO will result in a large growth stress within the TGO layer. When the growth stress reaches a certain value, cracks will form inside the TGO layer and/or near the interface between the TGO layer and the superalloy substrate or between the TGO layer and the YSZ top coat [2,12,13]. With the extension of service time, the crack propagation and aggregation will eventually lead to the failure of the YSZ top coat [13]. From this point of view, the service life of the TBCs can be improved by inhibiting the TGO layer growth.

Because the TGO layer growth determines the service life of the TBCs, much importance is attached to improving the oxidation resistance of MCrAlY bond coats. It's worth mentioning that adding reactive elements to bond coats is an effective way [2,14–16]. Although the specific mechanism is unknown, many studies have shown that the addition of Y, Hf, Pt, especially the Y element in the MCrAlY coatings can significantly reduce the TGO growth rate [2,14]. In addition, studies have shown that the oxidation resistance of the MCrAlY coatings prepared by different methods is obviously different. The bond coats prepared by atmospheric plasma spraying (APS), flame spraying (FS) and arc spraying (AS) usually have poor oxidation resistance due to the existence of more pores and oxides in the as-deposited coatings [17–19]. Since the bond coats deposited by electron beam physical vapor deposition (EB-PVD), high velocity oxygen fuel spraying (HVOF), low pressure plasma spraying (LPPS) or vacuum plasma spraying (VPS), multi-arc ion plating (MAIP), and cold gas dynamic spraying (CGDS) are more denser and less oxidized, the TGO layer growth rate of these coatings is slower [10,11,20–23]. After coating deposition, the oxidation resistance of MCrAlY bond coats prepared by the above advanced processes can be further improved by adopting some post-treatment processes. Many studies have shown that the oxidation resistance of MCrAlY bond coats can be effectively improved by using “blasting” (with ceramic grit), “peening” (with metallic particles), “media finishing” (in an abrasive slurry), pulsed electron beam treatment (PEB)

* Corresponding author.
E-mail address: ygj@mail.xjtu.edu.cn (G.-J. Yang).

https://doi.org/10.1016/j.surfcoat.2019.04.046
Received 26 February 2019; Received in revised form 9 April 2019; Accepted 13 April 2019
Available online 15 April 2019

and other post-treatment processes [24–27]. However, it should be noted that the above methods will inevitably introduce some impurity and/or change the surface morphology of coatings. For example, ceramic grit will introduce residue on the bond coat surface after "blasting" treatment, while "peening" and "media finishing" can reduce the surface roughness of the bond coats [28,29]. These will weaken the adhesion between the YSZ top coat and the MCrAlY bond coat and eventually lead to the early spalling failure of the YSZ top coat during service [10,11,22]. Therefore, it is necessary to develop new post-treatment approach to prepare highly oxidation resistant MCrAlY bond coats.

A novel heat treatment under low oxygen content was proposed in this study to improve the oxidation resistance of the MCrAlY coatings. The results showed that the growth of the TGO layer on the bond coat surface was significantly inhibited by the heat treatment. In order to explore the mechanisms of the improved oxidation resistance of heat-treated bond coats, the chemical composition of TGO, the grain structure of TGO, and the microstructure of the MCrAlY bond coats were characterized. Finally, the effects of the surface microstructure changes of MCrAlY bond coats on the TGO layer growth behavior were discussed.

2. Experimental procedures

2.1. Coating preparation

Nickel-based superalloy IN-738 (150 mm × 30 mm × 3 mm) was selected as the substrate. A commercial powder (Amdry 9951, Oerlikon Metco, Switzerland) with the nominal chemical composition of Co-31.7Ni-21.0Cr-8.0Al-0.5Y (wt%) was used for the MCrAlY bond coat deposition. The bond coat was deposited with a plasma torch (F6, GTV, Germany) in a vacuum chamber (MF-P 1000, GTV, Germany). The plasma spraying (LPPS and APS) parameters were listed in Table 1. After coating deposition, the coating was removed from the substrate surface, making the bond coat a free-standing coating.

2.2. Heat treatment under low oxygen content and isothermal oxidation treatment

Some of the as-deposited CoNiCrAlY bond coat samples were subjected to a heat treatment under low oxygen content in a vacuum furnace (SBF 966 H, EXEMOO, China). Prior to heating, the pressure in the furnace chamber was reduced to 10^{-3} Pa within 20 min, and then the furnace chamber was filled with high purity argon ($O_2 \leq 0.001$ ppm, Ar ≥ 99.999%) to a pressure of slightly above 1×10^5 Pa. This process of air pumping followed by gas filling was repeated for three times. The high purity argon with extremely low oxygen content filling into the furnace chamber can minimize oxygen content in the furnace. Moreover, a pressure of slightly above 1×10^5 Pa can prevent oxygen in the external environment from entering the chamber during heat treatment. This heat treatment under low oxygen content ($O_2 \leq 0.001$ ppm) did not lead to the oxidation of coatings during heat treatment [30]. Moreover, the surface microstructures of coatings changed significantly, which finally affected the growth behavior of TGO on the surface of bond coats during isothermal oxidation. These results could be observed in the next section. It should be noted that if the coating is oxidized during heat treatment, the surface microstructure changes of coatings during heat treatment and isothermal oxidation shown in Section 3 will not occur [31,32]. After the above operation has been completed, the specimens were heated to 1100 °C at a heating rate 4 °C/min and annealed at this temperature for 4 h. After that the samples were cooled to 25 °C at a cooling rate 4 °C/min in the furnace chamber. Finally, in a muffle furnace, the heat-treated bond coats and the as-deposited bond coats were isothermal oxidized for 4, 25, 64, 100, and 200 h at 1050 °C.

Table 1
Plasma spraying parameters.

Parameters	LPPS	APS
Arc current (A)	600	600
Arc voltage (V)	70	65
Primary plasma gas (Ar/slpm)	40	30
Secondary plasma gas (H_2/slpm)	7	5
Powder feed gas (Ar/slpm)	2	2
Spray distance (mm)	200	120
Traverse speed of torch (mm/s)	800	800

2.3. Microstructural characterization

The oxygen analyzer (ONH 836, LECO, USA) was used to measure the oxygen content of the CoNiCrAlY feedstock, the as-deposited bond coats, and the heat-treated bond coats. The chemical composition and microstructure of the CoNiCrAlY feedstock, the CoNiCrAlY bond coats, and the TGO layer were characterized by using EDS (GENESIS XM, EDAX, USA) and SEM (SU6600, Hitachi, Japan). In addition, the crystalline structure of the CoNiCrAlY feedstock, the CoNiCrAlY bond coats, and the TGO layer were characterized by using XRD (XRD-7000, SHIMADZU, Japan). The ImageJ software was used to measure the thicknesses of the TGO layer, the α-Al_2O_3 grain size, and the α-Al_2O_3 grain boundary density of bond coats. Before the measurement of cross-sections of the bond coats and the TGO layer, appropriate metallographic samples were prepared. A layer of nickel was deposited on the TGO layer surface using the chemical plating method due to protection of TGO layer from spalling off during preparation of metallographic specimens.

3. Results and discussion

3.1. Heat treatment exposing metallic phases without as-deposited alumina film to the coating surface

3.1.1. Surface microstructure changes of bond coats before and after heat treatment

Fig. 1(a) shows the surface microstructures of the as-deposited coatings. During the coating deposition, the melted feedstock particles transformed into smooth disk-shaped splats after they impacted on the superalloy substrate and previously deposited coating. As shown in Fig. 2, the oxygen content results showed that the oxygen content of the as-deposited bond coats was 0.164 wt%, which was around 3 times higher than that of the feedstock 0.051 wt%. This result confirms that the residual oxygen in the vacuum chamber reacted with the feedstock particles and finally formed an oxide film on the splat surface during the coating deposition. The existence of this oxide film was confirmed by the high resolution transmission electron microscopy (TEM) results of Choi [33] and Poza [34]. Moreover, the TEM results show the oxide film as amorphous alumina film, which is formed by the preferential oxidation of Al element in the feedstock and the rapid solidification of splat during the coating deposition [17,18,33,34]. In summary, there was an amorphous alumina film on the as-deposited CoNiCrAlY bond coat surface.

Fig. 1(c) shows the surface microstructures of the heat-treated coatings. The surface of the heat-treated splats was no longer smooth and the metallic grains were clearly visible. The phenomenon of surface faceting could be seen on the surface of some metallic grains [35]. Moreover, there were some black particles on the splat surface. The EDS results shown in Fig. 3 revealed that Al and O were present in large amounts in these black particles. This indicates that these black particles were alumina grains. It is worthwhile to note that the oxygen content of the heat-treated bond coats was 0.147 wt%, which was slightly less than that of the as-deposited bond coats 0.164 wt% (Fig. 2). This indicates that the coatings did not oxidized during heat treatment;

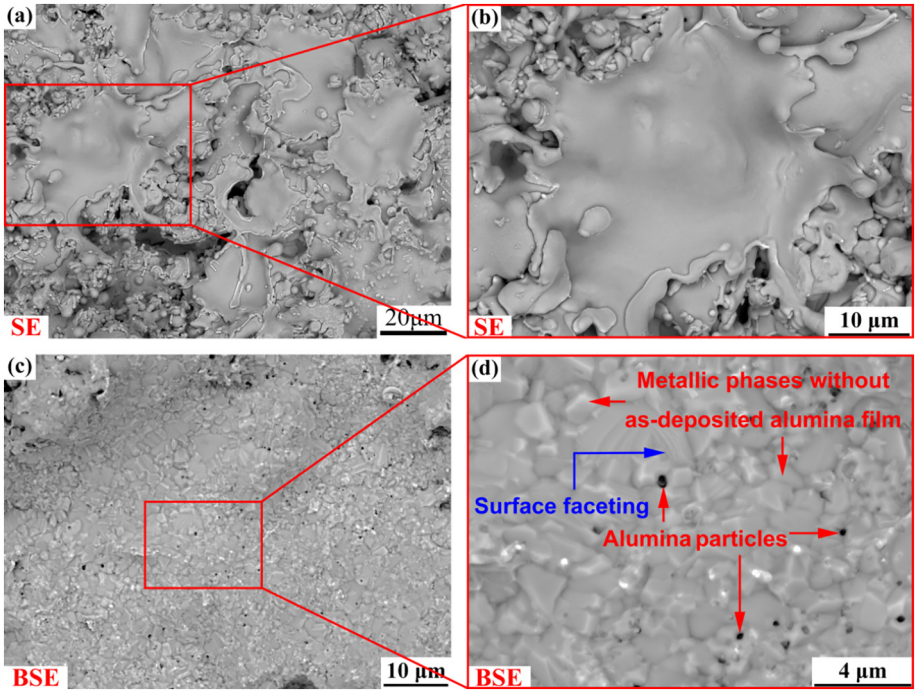

Fig. 1. Surface microstructures of the as-deposited CoNiCrAlY bond coats and the heat-treated CoNiCrAlY bond coats.

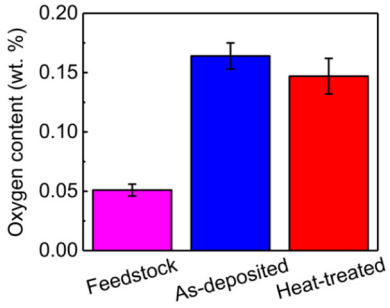

Fig. 2. Oxygen content of the CoNiCrAlY feedstock, the as-deposited bond coats, and the heat-treated bond coats.

on another way, these alumina grains were formed by the transformation of the amorphous alumina film. In order to figure out the process of transformation of amorphous alumina film into alumina grains during heat treatment, the same treatment was carried out on the CoNiCrAlY bond coats deposited by APS. It can be clearly seen in Fig. 4 after heat treatment, the thick alumina film on the surface of CoNiCrAlY coatings deposited in atmosphere agglomerated into alumina particles. Moreover, these agglomerated alumina particles were surrounded by metallic phases without as-deposited alumina film. The phenomenon of surface faceting could also be seen on the surface of some metallic grains. The above results indicate that the amorphous alumina film on the as-deposited bond coat surface agglomerated into alumina grains during the heat treatment under low oxygen content, which exposed

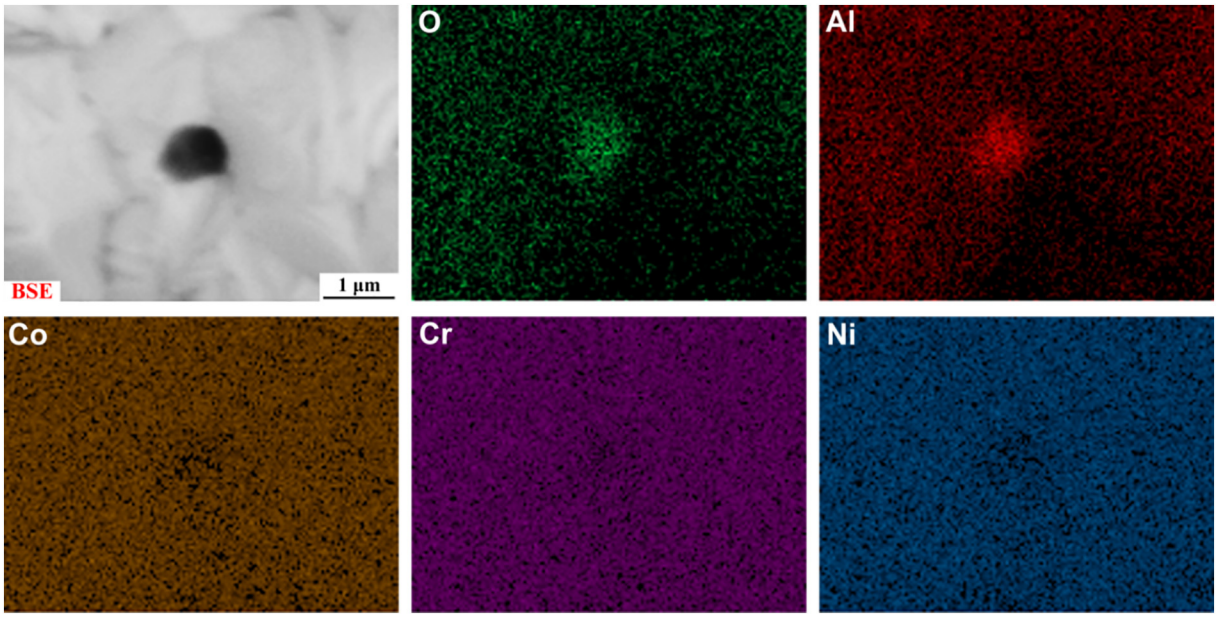

Fig. 3. EDS results of the heat-treated CoNiCrAlY bond coat surface.

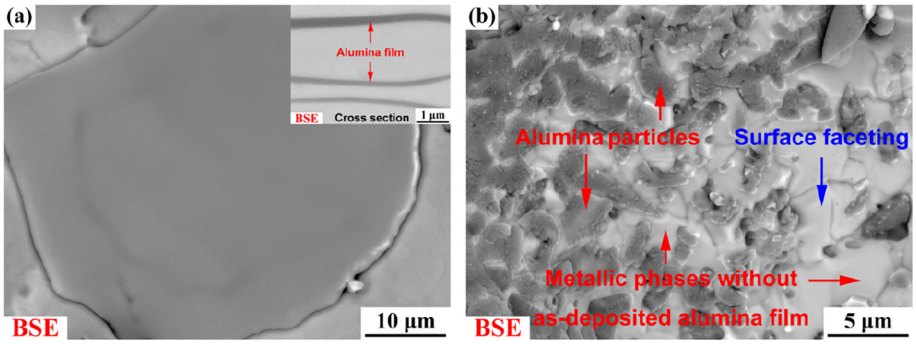

Fig. 4. Morphological changes of the alumina film on the surface of CoNiCrAlY bond coat deposited by APS: (a) as-deposited bond coats; (b) heat-treated bond coats.

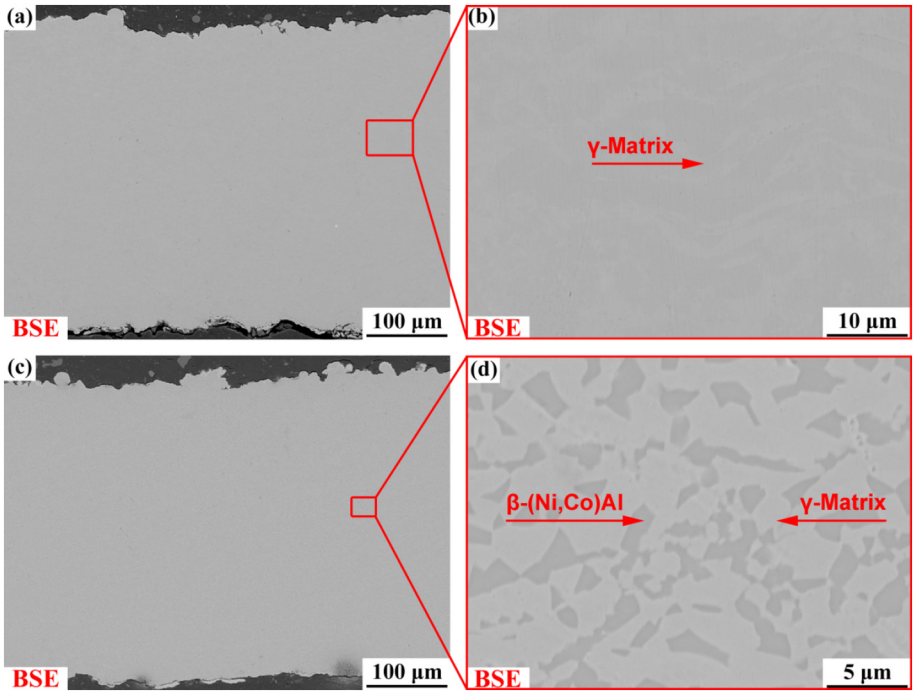

Fig. 5. Cross-sectional microstructures of the as-deposited CoNiCrAlY bond coats and the heat-treated CoNiCrAlY bond coats.

the metallic phases without as-deposited alumina film to the coating surface.

3.1.2. Microstructure changes within bond coats before and after heat treatment

Fig. 5(a) exhibits the cross-sectional microstructures of the as-deposited coatings. After adaptation of optimized parameters, the as-deposited bond coats were uniform and dense with a very low pore content of 0.1%. It could be seen from Fig. 5(b), as compared to the two-phase coexistence structure (β-(Ni,Co)Al + γ-matrix) of the feedstock powders (Fig. 6), there was only one phase (γ-matrix) in the as-deposited bond coats. This indicates that the β-(Ni,Co)Al of CoNiCrAlY feedstock powders dissolved into the γ-matrix during the coating deposition, and also, there was no precipitation of β-(Ni,Co)Al from this supersaturated γ-matrix during the subsequent solidification of CoNiCrAlY splats. In summary, the as-deposited CoNiCrAlY bond coats were dense coatings with a single-phase structure.

Fig. 5(c) exhibits the cross-sectional microstructures of the heat-treated coatings. The heat-treated bond coats were still uniform and dense compared to the as-deposited bond coats (Fig. 5(a)). As shown in Fig. 5(d), the heat-treated bond coats contained a two-phase coexistence structure. The XRD results showed that the phases in the heat-treated bond coats were β-(Ni,Co)Al and γ-matrix (Fig. 6). This

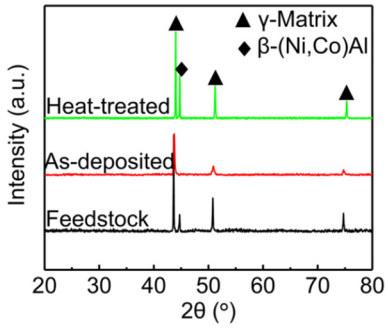

Fig. 6. XRD results of the CoNiCrAlY feedstock, the as-deposited bond coats, and the heat-treated bond coats.

indicates that the β-(Ni,Co)Al of the heat-treated bond coats was precipitated from the γ-matrix of the as-deposited bond coats during heat treatment. In summary, after the heat treatment under low oxygen content, the as-deposited bond coats with a single-phase structure transformed into coatings with a dual-phase structure.

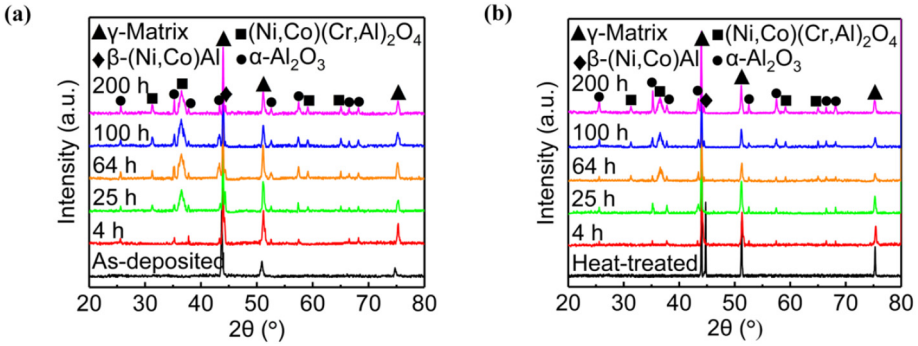

Fig. 7. XRD results of the CoNiCrAlY bond coats: (a) W/O HT bond coats; (b) W/HT bond coats.

3.2. Heat treatment reducing the TGO growth rate

Fig. 7 shows the XRD results of CoNiCrAlY bond coats after isothermal oxidation at 1050 °C for different durations. The bond coats without heat treatment (W/O HT bond coats) showed the α-Al_2O_3 peak after 4 h isothermal oxidation. Further 25 h isothermal oxidation, the (Co,Ni)(Cr,Al)$_2O_4$ peak appeared. In comparison, the bond coats with heat treatment (W/ HT bond coats) still had only the α-Al_2O_3 peak after 25 h isothermal oxidation, and the (Co,Ni)(Cr,Al)$_2O_4$ peak was only present after 64 h isothermal oxidation. In order to find out the specific causes of this phenomenon, we further examined the cross-sectional microstructures of the TGO layer after isothermal oxidation in air at 1050 °C for different durations.

Fig. 8 shows the cross-sectional microstructures of the TGO layer. It could be clearly seen from Fig. 8(a) and (b), the TGO on the surface of these CoNiCrAlY bond coats was monolayer TGO after 4 h isothermal oxidation. The EDS results (Fig. 9(a)) showed that this monolayer TGO contains only the Al and O elements, which indicates that this single-layer TGO was α-Al_2O_3 TGO. This was consistent with the XRD results of Fig. 7. When the isothermal oxidation time was extended to 25 h, the TGO of the W/O HT bond coats consisted of two layers, while the W/ HT bond coats had only one layer of TGO. The EDS results (Fig. 9(b)) showed that the inner TGO layer contains only the O and Al elements, while the outer TGO layer contains a large amount of O, Al, Co, and Cr elements. This indicates that the inner TGO layer was α-Al_2O_3 and the outer TGO layer was (Co,Ni)(Cr,Al)$_2O_4$. This was also consistent with the XRD results of Fig. 7. When the isothermal oxidation time exceeded 64 h, the TGO layer of these two types of bond coats divided into two layers. The inner layer was α-Al_2O_3 TGO and the outer layer was (Co,Ni)(Cr,Al)$_2O_4$ TGO. It is noteworthy that the (Co,Ni)(Cr,Al)$_2O_4$ TGO had more pores, while the α-Al_2O_3 TGO was dense. Another obvious feature was noted, while the time of isothermal oxidation increased, the TGO layer gradually thickened. However, the TGO layer thickness of the W/O HT bond coats was obviously higher than that of the W/ HT bond coats. The relationship between the isothermal oxidation time and the TGO layer thickness was shown in Fig. 10. Apparently, the growth of the TGO layer substantially conform the parabolic growth law. However, the W/O HT bond coats had a parabolic growth rate constant 0.28 μm/$h^{1/2}$, while the W/ HT bond coats had a parabolic growth rate constant 0.17 μm/$h^{1/2}$. Since the TGO layer had a critical thickness during TBCs service, the lifetime of TBCs was usually judged by the oxidation time under the same TGO layer thickness [12]. From this point of view, the oxidation time for the same TGO thickness of the W/ HT bond coats was 2.7 times slower than that of the W/O HT bond coats. The above results indicate that the heat treatment under low oxygen content significantly inhibited the TGO layer growth.

3.3. Heat treatment promoting the formation of α-Al_2O_3 TGO with large grain size

In order to explore the mechanisms for the slow growth of the TGO layer on the W/ HT bond coat surface, we further characterized the TGO grain structure. Fig. 7 and Fig. 8 have shown that α-Al_2O_3 was first formed during isothermal oxidation. As the isothermal oxidation time increases, (Co,Ni)(Cr,Al)$_2O_4$ was formed on α-Al_2O_3 surface. It is generally believed that the α-Al_2O_3 TGO growth was controlled by the inward diffusion of oxygen ions, while the (Co,Ni)(Cr,Al)$_2O_4$ TGO growth was dominated by the outward diffusion of metal ions [2,36]. Since the (Co,Ni)(Cr,Al)$_2O_4$ TGO generally contained a large amount of pores and the diffusion of oxygen ions in the (Co,Ni)(Cr,Al)$_2O_4$ was much easier than that of α-Al_2O_3, the (Co,Ni)(Cr,Al)$_2O_4$ TGO was a good conductor of oxygen ions [2,5,10]. Therefore, the inner layer α-Al_2O_3 TGO growth rate was mainly controlled by the diffusion rate of oxygen ions in the α-Al_2O_3. On the other hand, since the metal ions needed for the growth of the outer (Co,Ni)(Cr,Al)$_2O_4$ TGO must first pass through the inner layer of α-Al_2O_3, the diffusion rate of metal ions in α-Al_2O_3 TGO would be the key to determining the growth rate of outer (Co,Ni)(Cr,Al)$_2O_4$ TGO. Therefore, the diffusion rate of ions in the inner α-Al_2O_3 TGO was the key to determining the entire TGO layer growth rate. According to the high temperature oxidation theory of metal or alloy, the diffusion rate of the ions in the oxide film was mainly affected by the oxidation temperature, the properties of diffusion ions, and the diffusion channels [37]. The diffusion channel was the key to controlling the growth rate of oxide film under the certain conditions of oxidation temperature and diffusion ions. Previous studies have shown that the diffusion coefficient of ions through bulk diffusion was about several orders of magnitude smaller than that of through grain boundaries [38]. Therefore, the number of grain boundaries has a significant effect on the oxide film growth rate.

To explore the effect of the heat treatment under low oxygen content on the TGO layer growth rate, it is necessary to characterize the number of grain boundaries of the inner α-Al_2O_3 TGO layer. Since we can indirectly know the number of grain boundaries by characterizing the grain size, we need to accurately measure the α-Al_2O_3 grain size. In this study, the α-Al_2O_3 grain size was directly observed by peeling off the entire TGO layer from the CoNiCrAlY bond coat surface (Fig. 11) [10]. Fig. 12 shows the α-Al_2O_3 grain size next to the interface between the CoNiCrAlY bond coats and the α-Al_2O_3 TGO layer. The α-Al_2O_3 grain size has been calculated as shown in Fig. 13. With maintain same isothermal oxidation time, the α-Al_2O_3 grain of W/ HT bond coats was larger than that of W/O HT bond coats (Fig. 13(a)). In addition, the α-Al_2O_3 grain size increased with the increase of the isothermal oxidation time, which was caused by the grain coarsening during the isothermal oxidation. Furthermore, the α-Al_2O_3 grain boundary density was quantitatively analyzed as shown in Fig. 13(b). Apparently, the α-Al_2O_3 grain boundary density of the W/O HT bond coats was larger than that of the W/ HT bond coats.

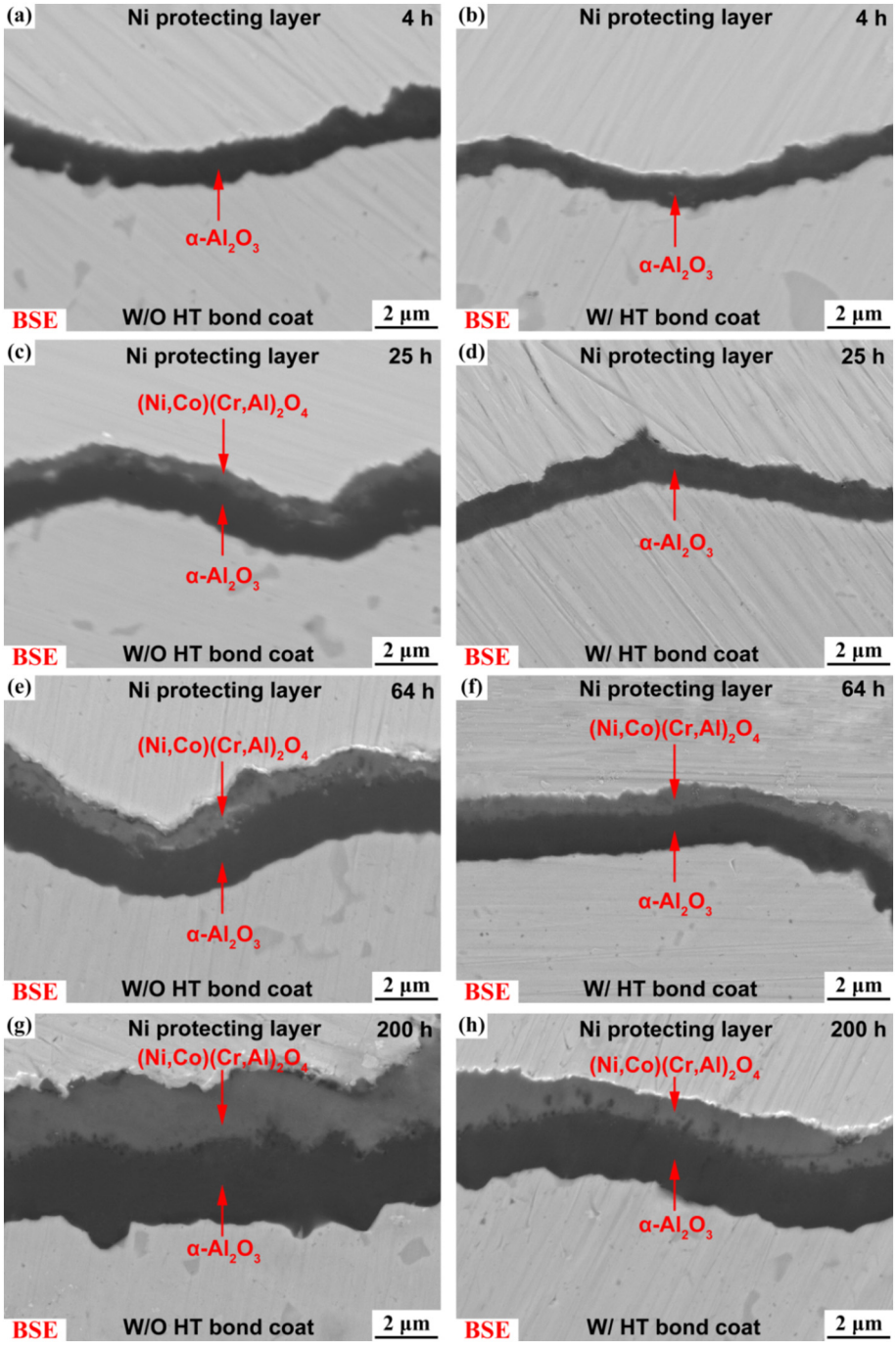

Fig. 8. Cross-sectional microstructures of the TGO layer: (a), (c), (e), (g) W/O HT bond coats; (b), (d), (f), (h) W/HT bond coats.

3.4. Mechanism on heat treatment reducing the TGO growth rate

In general, the TGO grain growth behavior is strongly influenced by the initial surface microstructures of the bond coats [24–27]. In this study, under the same conditions of isothermal oxidation, the difference between the TGO growth behaviors of these two kinds of bond coats was related to the different surface microstructures of coatings. Fig. 1(a), Fig. 2 and Fig. 4(a) have shown that the as-deposited bond coat surface was covered with an amorphous alumina film. However, during the heat treatment under low oxygen content, this amorphous alumina film agglomerated into alumina particles (Fig. 1(d) and Fig. 4(b)). This change in morphology of the alumina film led to the exposure of the metallic phases without as-deposited alumina film. In this section, the effect of alumina film morphology change on the α-Al_2O_3 TGO growth behavior was discussed.

Fig. 14(a) is the schematic diagram of the α-Al_2O_3 TGO growth process on the W/O HT bond coat surface. In the initial stage of oxidation, since the as-deposited bond coat surface was covered by an amorphous alumina film, what happens first was the microstructure change of this alumina film. Studies have shown that the amorphous alumina film on the alloy surface would be transformed into alumina crystal film with an average grain size of several nanometers during high temperature oxidation [39]. Therefore, in the early stage of isothermal oxidation, the growth of the α-Al_2O_3 TGO was based on the fine-grained alumina film. With increasing the isothermal oxidation time, α-Al_2O_3 TGO would grow thicker and the α-Al_2O_3 grains would merge with each other. Therefore, in the middle stage of isothermal oxidation, the α-Al_2O_3 grain size was obviously larger than that of in

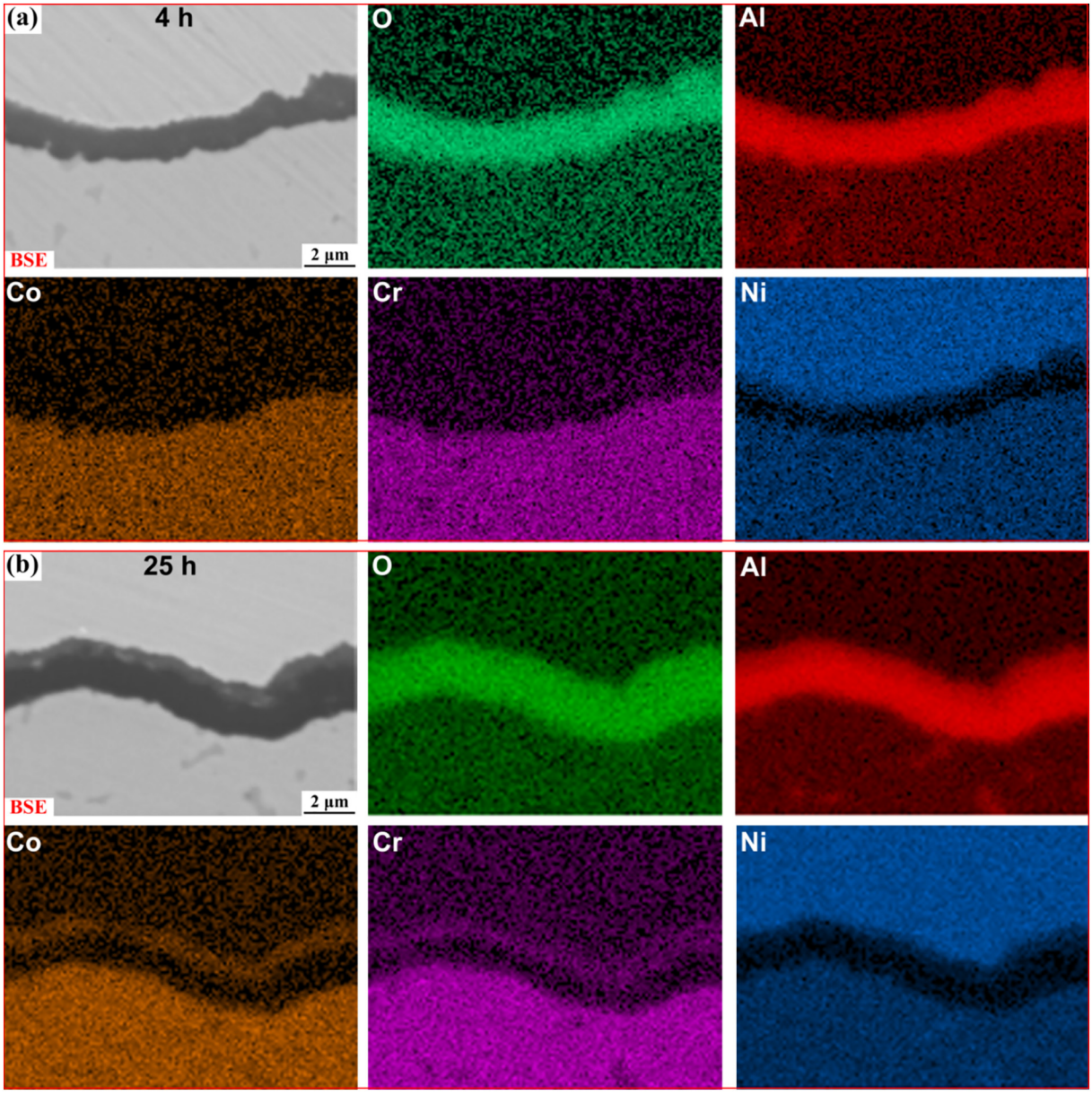

Fig. 9. EDS results of the TGO layer on the W/O HT bond coat surface: (a) 4 h; (b) 25 h.

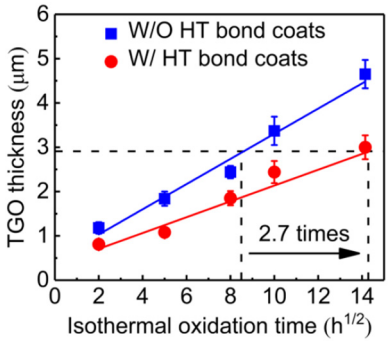

Fig. 10. Isothermal oxidation kinetics curves of the W/O HT bond coats and W/ HT bond coats.

the early stage of isothermal oxidation. It should be pointed out that the α-Al_2O_3 grain size of the W/ HT bond coats in each oxidation stage was larger than that of the W/O HT bond coats. Therefore, as we described in the Section 3.3, the α-Al_2O_3 TGO growth rate of W/O HT bond coats was higher than that of the W/ HT bond coats. The grain size or grain boundary density of the inner α-Al_2O_3 TGO had the same effect on the growth rate of the outer $(Co,Ni)(Cr,Al)_2O_4$ TGO layer. Therefore, the entire TGO growth rate of the W/O HT bond coats was larger than that of the W/ HT bond coats. In summary, because of the smaller grain size of α-Al_2O_3 formed in the early stage of isothermal oxidation, the TGO layer growth rate of the W/O HT bond coats was larger than that of the W/ HT bond coats.

Fig. 14(b) is the schematic diagram of the α-Al_2O_3 TGO growth process on the W/ HT bond coat surface. During the heat treatment under low oxygen content, the amorphous alumina film formed on the surface of the as-deposited CoNiCrAlY bond coats gradually broke down and subsequently shrank into alumina particles. This morphological change of the alumina film was caused by the agglomeration of the amorphous alumina film [40]. The agglomeration of the amorphous alumina film resulted in the exposure of metallic phases without as-deposited alumina film on the W/HT bond coat surface. In the early stage of isothermal oxidation, a layer of α-Al_2O_3 TGO would be formed

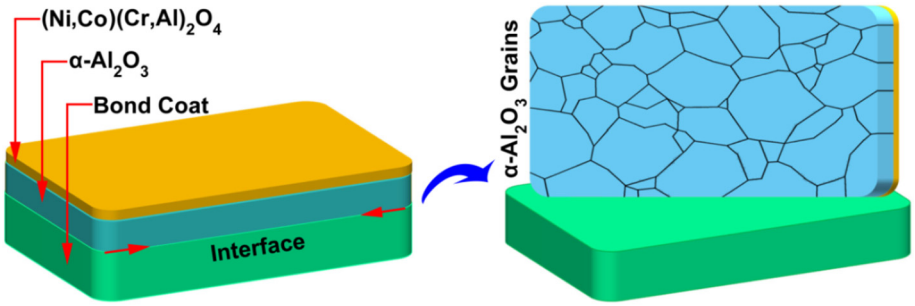

Fig. 11. Schematic diagram of the operation process for obtaining the α-Al_2O_3 grain size next to the interface between the α-Al_2O_3 TGO layer and the CoNiCrAlY bond coats.

through nucleation and growth process on the surface of these metallic phases without as-deposited alumina film. However, it should be noted that the grain size of the α-Al_2O_3 TGO formed through nucleation and growth process was larger than that of the α-Al_2O_3 TGO formed by the crystallization of the amorphous alumina film. The specific reasons may be related to the surface microstructure changes of the bond coats during heat treatment such as the phase structure change of the coatings (Fig. 5 and Fig. 6) and the surface faceting of bare metallic phases (Fig. 1 and Fig. 4). The surface of β-(Ni,Co)Al phase and/or the surface of bare metallic phases with faceting phenomenon may be unfavorable to the nucleation of α-Al_2O. As a result, the α-Al_2O_3 grain boundary density of the W/O HT bond coats was larger than that of the W/ HT bond coats. The larger α-Al_2O_3 grain size or the smaller α-Al_2O_3 grain boundary density finally resulted in a smaller TGO layer growth rate. At this stage we can suggest that if we want to reduce the TGO layer growth rate, it is necessary to properly adjust the surface microstructures of the bond coats to aim of preparing a large-grains α-Al_2O_3 film in the early stage of isothermal oxidation. In summary, because of the larger grain size of α-Al_2O_3 formed in the early stage of isothermal oxidation, the growth rate of the TGO layer on the W/ HT bond coat surface was smaller than that of the W/O HT bond coats.

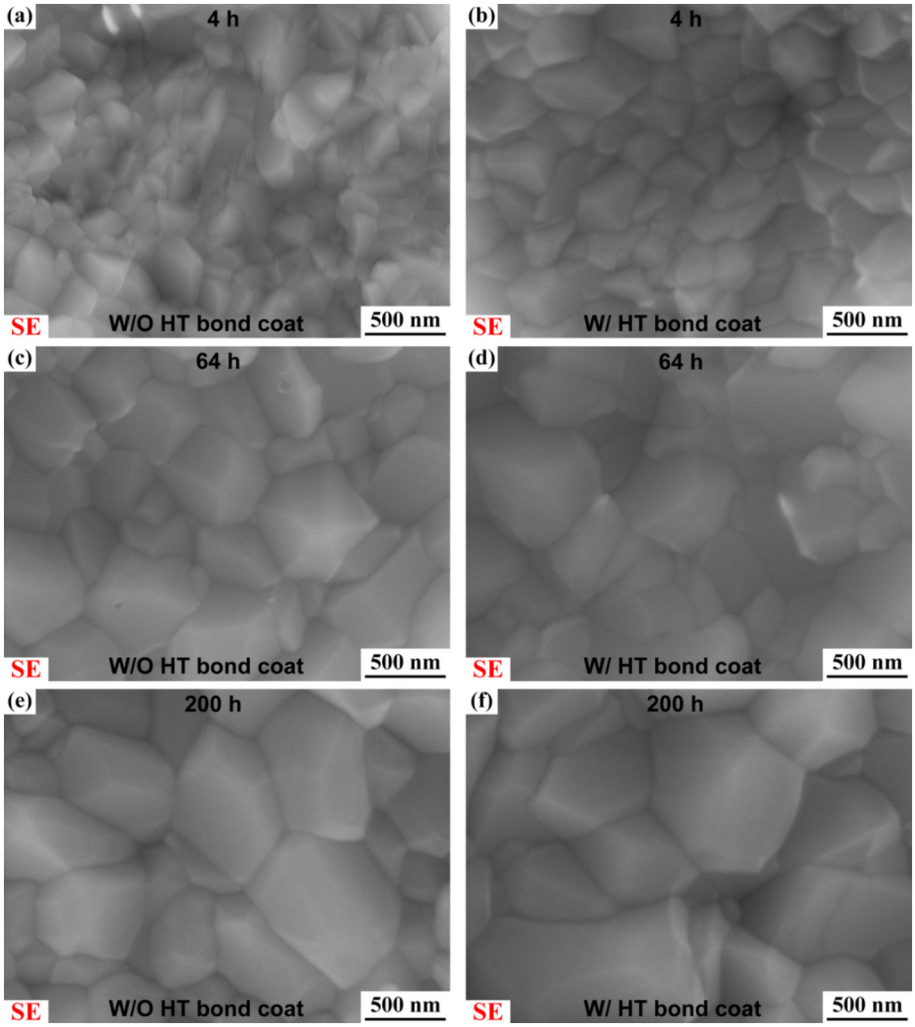

Fig. 12. α-Al_2O_3 grain size next to the interface between the α-Al_2O_3 TGO layer and the CoNiCrAlY bond coats: (a), (c), (e) W/O HT bond coats; (b), (d), (f) W/ HT bond coats.

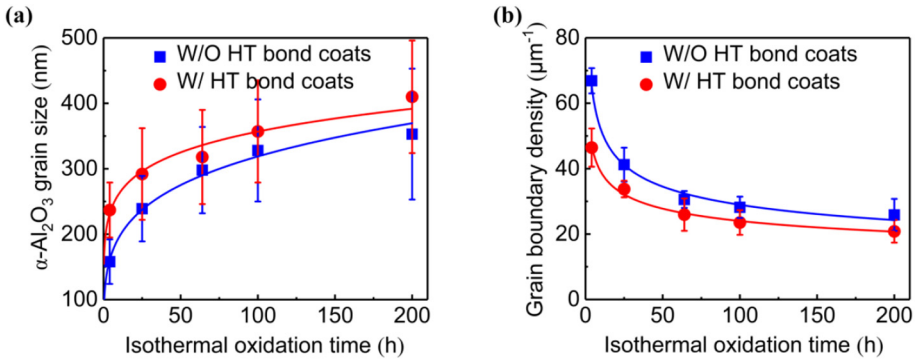

Fig. 13. α-Al_2O_3 grain size and α-Al_2O_3 grain boundary density of the CoNiCrAlY bond coats: (a) grain size; (b) grain boundary density.

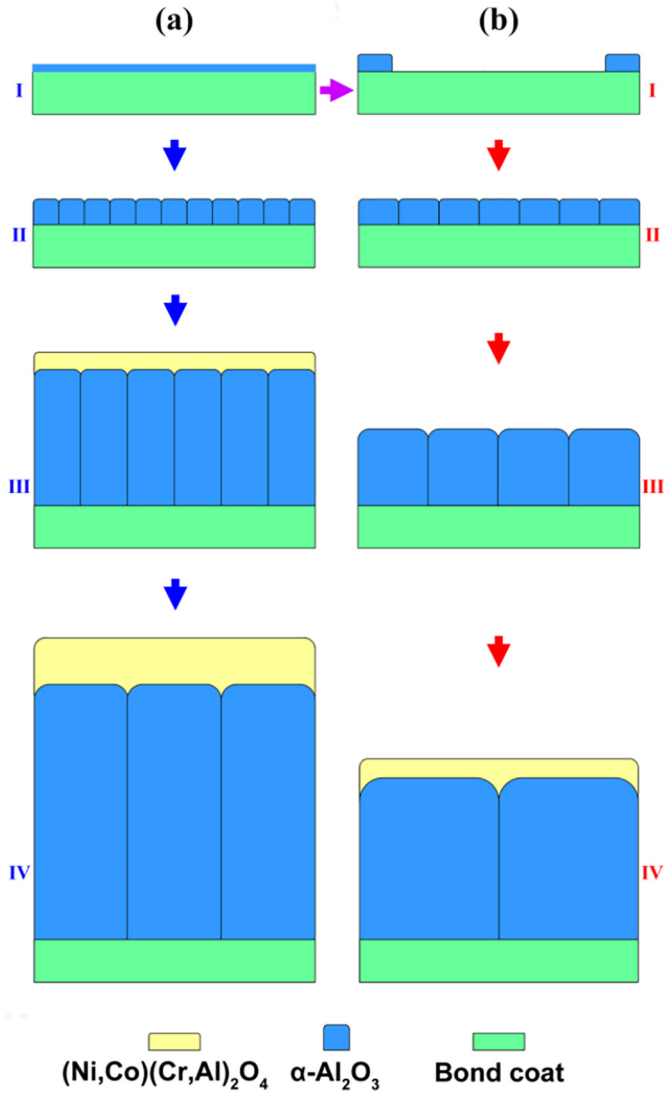

Fig. 14. Schematic diagram of the α-Al_2O_3 TGO growth process on the surface of CoNiCrAlY bond coats during isothermal oxidation: (a) W/O HT bond coats; (b) W/HT bond coats.

4. Conclusions

In this study, the heat treatment under low oxygen content significantly inhibited the TGO layer growth and improved the oxidation resistance of the CoNiCrAlY bond coats. The following are the conclusions:

1. The heat treatment under low oxygen content exposed the metallic phases without as-deposited alumina film to the coating surface.
2. During isothermal oxidation, the α-Al_2O_3 grain size of the W/HT bond coats was larger than that of the W/O HT bond coats.
3. The W/O HT bond coats had a parabolic growth rate constant 0.28 μm/$h^{1/2}$, while the W/HT bond coats had a parabolic growth rate constant 0.17 μm/$h^{1/2}$.
4. The oxidation time for the same TGO thickness of the W/HT bond coats was 2.7 times slower than that of the W/O HT bond coats.

Acknowledgments

This work was supported by the National Science Foundation of China [Grant No. 51671159]; the Fundamental Research Funds for the Central Universities; and the National Program for Support of Top-notch Young Professionals.

References

[1] N.P. Padture, Advanced structural ceramics in aerospace propulsion, Nat. Mater. 15 (2016) 804–809.
[2] N.P. Padture, M. Gell, E.H. Jordan, Thermal barrier coatings for gas-turbine engine applications, Science 296 (2002) 280–284.
[3] R. Kromer, J. Cormier, S. Costil, D. Courapied, L. Berthe, P. Peyre, High temperature durability of a bond-coatless plasma-sprayed thermal barrier coating system with laser textured Ni-based single crystal substrate, Surf. Coat. Technol. 337 (2018) 168–176.
[4] R. Kumar, D. Cietek, C. Jiang, J. Roth, M. Gell, E.H. Jordan, Influence of microstructure on the durability of gadolinium zirconate thermal barrier coatings using APS & SPPS processes, Surf. Coat. Technol. 337 (2018) 117–125.
[5] D.R. Clarke, M. Oechsner, N.P. Padture, Thermal-barrier coatings for more efficient gas-turbine engines, MRS Bull. 37 (2012) 891–898.
[6] S.Y. Cui, Q. Miao, W.P. Liang, B.Q. Li, Oxidation behavior of NiCoCrAlY coatings deposited by double-glow plasma alloying, Appl. Surf. Sci. 428 (2018) 781–787.
[7] K. Torkashvand, E. Poursaeidi, Effect of temperature and ceramic bonding on BC oxidation behavior in plasma-sprayed thermal barrier coatings, Surf. Coat. Technol. 349 (2018) 177–185.
[8] R. Ghasemi, Z. Valefi, The effect of the Re-Ni diffusion barrier on the adhesion strength and thermal shock resistance of the NiCoCrAlY coating, Surf. Coat. Technol. 344 (2018) 359–372.
[9] G.R. Li, L.S. Wang, Durable TBCs with self-enhanced thermal insulation based on co-design on macro- and microstructure, Appl. Surf. Sci. doi:https://doi.org/10.1016/j.apsusc.2019.03.309.
[10] B.Y. Zhang, G.J. Yang, C.X. Li, C.J. Li, Non-parabolic isothermal oxidation kinetics of low pressure plasma sprayed MCrAlY bond coat, Appl. Surf. Sci. 406 (2017) 99–109.
[11] B.Y. Zhang, G.H. Meng, G.J. Yang, C.X. Li, C.J. Li, Dependence of scale thickness on the breaking behavior of the initial oxide on plasma spray bond coat surface during vacuum pre-treatment, Appl. Surf. Sci. 397 (2017) 125–132.
[12] H. Dong, G.J. Yang, C.X. Li, X.T. Luo, C.J. Li, Effect of TGO thickness on thermal cyclic lifetime and failure mode of plasma-sprayed TBCs, J. Am. Ceram. Soc. 97 (2014) 1226–1232.
[13] A.G. Evans, D.R. Mumm, J.W. Hutchinson, G.H. Meier, F.S. Pettit, Mechanisms controlling the durability of thermal barrier coatings, Prog. Mater. Sci. 46 (2001) 505–553.
[14] C.S. Zhao, Y.H. Zhou, Z.H. Zou, L.R. Luo, X.F. Zhao, F.W. Guo, P. Xiao, Effect of alloyed Lu, Hf and Cr on the oxidation and spallation behavior of NiAl, Corros. Sci. 126 (2017) 334–343.
[15] D.K. Das, Microstructure and high temperature oxidation behavior of Pt-modified

aluminide bond coats on Ni-base superalloys, Prog. Mater. Sci. 58 (2013) 151–182.
[16] Y.F. Yang, C.Y. Jiang, H.R. Yao, Z.B. Bao, S.L. Zhu, F.H. Wang, Preparation and enhanced oxidation performance of a Hf-doped single-phase Pt-modified aluminide coating, Corros. Sci. 113 (2016) 17–25.
[17] G.H. Meng, B.Y. Zhang, H. Liu, G.J. Yang, T. Xu, C.X. Li, C.J. Li, Vacuum heat treatment mechanisms promoting the adhesion strength of thermally sprayed metallic coatings, Surf. Coat. Technol. 344 (2018) 102–110.
[18] G.H. Meng, B.Y. Zhang, H. Liu, G.J. Yang, T. Xu, C.X. Li, C.J. Li, Highly oxidation resistant and cost effective MCrAlY bond coats prepared by controlled atmosphere heat treatment, Surf. Coat. Technol. 347 (2018) 54–65.
[19] R.R. Chen, X. Gong, Y. Wang, G. Qin, N.N. Zhang, Y.Q. Su, H.S. Ding, J.J. Guo, H.Z. Fu, Microstructure and oxidation behaviour of plasma-sprayed NiCoCrAlY coatings with and without Ta on Ti44Al6Nb1Cr alloys, Corros. Sci. 136 (2018) 244–254.
[20] J.L. Wang, M.H. Chen, Y.X. Cheng, L.L. Yang, Z.B. Bao, L. Liu, S.L. Zhu, F.H. Wang, Hot corrosion of arc ion plating NiCrAlY and sputtered nanocrystalline coatings on a nickel-based single-crystal superalloy, Corros. Sci. 123 (2017) 27–39.
[21] A.C. Karaoglanli, A. Turk, Isothermal oxidation behavior and kinetics of thermal barrier coatings produced by cold gas dynamic spray technique, Surf. Coat. Technol. 318 (2017) 72–81.
[22] B.Y. Zhang, J. Shi, G.J. Yang, C.X. Li, C.J. Li, Healing of the interface between splashed particles and underlying bulk coating and its influence on isothermal oxidation behavior of LPPS MCrAlY bond coat, J. Therm. Spray Technol. 24 (2015) 611–621.
[23] M.J. Lance, J.A. Haynes, B.A. Pint, Performance of vacuum plasma spray and HVOF bond coatings at 900° and 1100 °C, Surf. Coat. Technol. 337 (2018) 136–140.
[24] F. Naeimi, M.R. Rahimipour, M. Salehi, Effect of sandblasting process on the oxidation behavior of HVOF MCrAlY coatings, Oxid. Met. 86 (2016) 59–73.
[25] S.F. Zhou, Z. Xiong, J.B. Lei, X.Q. Dai, T.Y. Zhang, C.X. Wang, Influence of milling time on the microstructure evolution and oxidation behavior of NiCrAlY coatings by laser induction hybrid cladding, Corros. Sci. 103 (2016) 105–116.
[26] R.G. Wellman, A. Scrivani, G. Rizzi, A. Weisenburger, F.H. Tenailleau, J.R. Nicholls, Pulsed electron beam treatment of MCrAlY bondcoats for EB-PVD TBC systems part 2 of 2: cyclic oxidation of the coatings, Surf. Coat. Technol. 202 (2007) 709–713.
[27] T.J. Nijdam, L.P.H. Jeurgens, J.H. Chen, W.G. Sloof, On the microstructure of the initial oxide grown by controlled annealing and oxidation on a NiCoCrAlY bond coating, Oxid. Met. 64 (2005) 355–377.
[28] L. Pawlowski, The Science and Engineering of Thermal Spray Coatings, John Wiley & Sons, 2008.
[29] P.L. Fauchais, J.V.R. Heberlein, M.I. Boulos, Thermal Spray Fundamentals, Springer US, 2014.
[30] H. Qin, X. Chen, J. Li, P. Sutter, G. Zhou, Atomic-step-induced local nonequilibrium effects on surface oxidation, J. Phys. Chem. C 121 (2017) 22846–22853.
[31] A. Gil, D. Naumenko, R. Vassen, J. Toscano, M. Subanovic, L. Singheiser, W.J. Quadakkers, Y-rich oxide distribution in plasma sprayed MCrAlY-coatings studied by SEM with a cathodoluminescence detector and Raman spectroscopy, Surf. Coat. Technol. 204 (2009) 531–538.
[32] L.W. Zhang, L. Lu, L. Wang, X.J. Ning, Q.S. Wang, R.X. Wang, Microstructural characteristics and oxidation behavior of low-pressure cold-sprayed CoNiCrAlY coatings, J. Therm. Spray Technol. 26 (2017) 1565–1572.
[33] H. Choi, B. Yoon, H. Kim, C. Lee, Isothermal oxidation of air plasma spray NiCrAlY bond coatings, Surf. Coat. Technol. 150 (2002) 297–308.
[34] P. Poza, J. Gómez-García, C.J. Múnez, TEM analysis of the microstructure of thermal barrier coatings after isothermal oxidation, Acta Mater. 60 (2012) 7197–7206.
[35] G. Zhou, W. Liang, J.C. Yang, Effect of surface topology on the formation of oxide islands on Cu surfaces, J. Appl. Phys. 97 (2005) 063509.
[36] R. Prescott, M.J. Graham, The formation of aluminum oxide scales on high-temperature alloys, Oxid. Met. 38 (1992) 233–254.
[37] N. Birks, G.H. Meier, F.S. Pettit, Introduction to the High-Temperature Oxidation of Metals, 2nd ed., Cambridge University Press, New York, 2006.
[38] K. Messaoudi, A.M. Huntz, B. Lesage, Diffusion and growth mechanism of Al_2O_3 scales on ferritic Fe-Cr-Al alloys, Mater. Sci. Eng. A 247 (1998) 248–262.
[39] H.L. Qin, P. Sutter, G.W. Zhou, The crystallization of amorphous aluminum oxide thin films grown on NiAl(100), J. Am. Ceram. Soc. 97 (2014) 2762–2769.
[40] C.V. Thompson, Solid-state dewetting of thin films, Annu. Rev. Mater. Res. 42 (2012) 399–434.